

Electrostatic model to understand the influence of salt deposit in GFRP material during lightning discharges

Sathiesh Kumar V * Nilesh J Vasa** and Sarathi R***

A methodical experimentation and mathematical modeling is carried out to study the influence of salt deposit on wind turbine blade material (Glass Fiber Reinforced Plastics/GFRP) during lightning discharges. Electrical discharge measurements combined with optical emission spectroscopy technique and electrostatics is utilized to understand the dynamics of surface discharge and the level of damage on GFRP material. COMSOL simulation studies shows that the electric field intensity on the surface of the polluted GFRP gets enhanced when compared to that of virgin GFRP, irrespective of the applied voltage profile and polarity. Flashover voltage, discharge current and optical emission spectroscopy measurements indicates that the deterioration of GFRP material is severe when there is an adhesion of salt deposit. It is also observed that the damage induced on GFRP material is severe for winter lightning (switching impulse voltage of 250/2500 μ s) compared to that of summer lightning (lightning impulse voltage of 1.2/50 μ s) due to a longer front and tail period of the pulse.

Keywords: *Wind blade, pollution measurement, flashover voltage, lightning impulse, switching impulse, temporal and spatial measurements.*

1.0 INTRODUCTION

The world over researchers are trying to maximize the power handling capability of wind turbine structure by increasing the blade swept area and also by installing the turbines in regions of high wind velocity such as offshore and mountain regions. In an offshore environment, lightning damages to wind turbine blades (made from glass fiber reinforced plastics (GFRP) material) are increasing as the number and size of installed wind turbines are rapidly becoming larger. The damage caused to a blade is quite serious since the cost for replacements are remarkably high and long repair time is necessary. Even though preventive measures, such as using metallic cap receptors, have been utilized near the blade tip, still lightning damages to wind turbines remains a major concern. One of the reasons may be due

to the accumulation of a pollutant layer (salt) on wind turbine blade and results in the reduction of dielectric breakdown strength of the material. As a result, lightning can strike any part of the blade other than the receptors. The polluted surface with higher conductivity can allow discharge current to propagate over the surface and may result in damage of the blade. On the other hand, studies on influence of salt deposit on outdoor insulators in the coastal regions and its electrical characteristics are available in extensive [1-13].

In this work, an attempt has been made to understand the influence of surface pollutant, such as salt deposit, on wind turbine blade material under transient voltages. Pollution (NaCl) deposition on GFRP material is carried out as per IEC 60507 standards (Standard used for testing high voltage equipment in an offshore environment) [14].

*Department of Electronics Engineering, Madras Institute of Technology, Anna University, Chennai- 600044, India.

**Department of Engineering Design, Indian Institute of Technology Madras, Chennai- 600036, India.

***Department of Electrical Engineering, Indian Institute of Technology Madras, Chennai- 600036, India.

Electrical discharge measurement combined with optical emission spectroscopy (OES) technique is used to study the dynamics of surface discharge and the level of damage on GFRP material under lightning impulse voltage (1.2/50 μ s) and switching impulse voltage (250/2500 μ s), respectively. Lightning impulse and switching impulse voltage depicts the characteristics of summer and winter lightning, respectively [15]. Also theoretical modeling is carried out to understand the electrostatic phenomenon during lightning discharges.

2.0 EXPERIMENTAL ANALYSIS

2.1 Preparation of Test Specimen

Commercially available woven fabric glass fiber reinforced plastic material with a surface area of 36cm² is selected for the present study. The literature, regarding the amount of salt deposition on wind turbine blades in an offshore environment is limited. Also there are no standards for estimating or understanding the pollution performance of wind turbine blade structures due to lightning. Hence, the methodology adopted for characterizing pollution performance of outdoor insulators is followed [14]. Salt deposit density (SDD) on GFRP sample considered in the study varies from 0 to 11mg/cm² which is in accordance with density used in testing of high voltage insulators in an offshore environment. As per the IEC 60507 standard, solid layer method is used for depositing the pollutant on the surface of GFRP material [14]. Slurry is prepared by mixing kaolin clay (acts as a binding medium) and NaCl in different proportions with de-ionized water and sprayed over the surface of glass fiber to form a thin layer.

2.2 Optical Emission Spectroscopy (OES) technique

Standards define the impulse voltage as a unidirectional voltage which rises more or less rapidly to a peak value and then decays relatively slowly to zero [16],[17]. Summer and winter lightning characteristics are different. Duration of

the current flow due to winter lightning is longer than that of summer lightning. Hence lightning impulse (LI) voltage wave of 1.2/50 μ s and switching impulse (SI) voltage wave of 250/2500 μ s, represent summer and winter lightning are used in the present study.

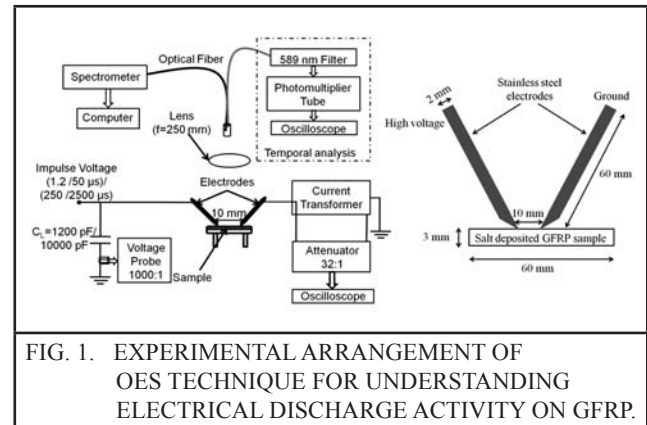


FIG. 1. EXPERIMENTAL ARRANGEMENT OF OES TECHNIQUE FOR UNDERSTANDING ELECTRICAL DISCHARGE ACTIVITY ON GFRP.

Figure 1 show an experimental setup of optical emission spectroscopy technique for understanding the dynamics of surface discharge activity under transient voltages. GFRP sample (3 mm thick) with the SDD ranging from 0 to 11mg/cm² are used. To produce quasi uniform electric field gap, the test electrode gap consist of two angular stainless steel electrodes tip cut for 45°(with edges smooth) placed on the GFRP sample (as per IEC 60112 [18]). Also this electrode configuration allows uniform electric field to develop on the polluted GFRP to initiate the surface discharge process. The two electrodes are separated by a gap distance of 10mm. Voltage probe (EP-50k, PEEC.A, LeCroy, 1000:1) and a current probe (94111-1, ETS Lindgren) combined with attenuator (resistive shunt, 32:1) are used to measure the applied voltage and discharge current, respectively. Lens with a focal length of 250mm is used for collecting the optical emission during the discharge process and it is coupled to a spectrometer (190 to 1035 nm, Tec5) with an NMOS linear image sensor (S3901, Hamamatsu) using a multimode optical fiber (core radius and a NA of 300 μ m and 0.39). To perform discharge plasma emission lifetime studies, neutral sodium atom (Na I, D-line, 588.99 nm) emission line is used. Na I emission line is filtered using a sodium band-pass filter (589 nm, FWHM=10 nm) and focused on to a multimode optical

fiber which is coupled to a photomultiplier tube (R562, Hamamatsu Photonics, Time resolution of 45ns). The output from the photomultiplier tube is connected to a high bandwidth oscilloscope (LeCroy, 1GHz, 4 Channel, 1GS/s).

2.3 Results and Discussion

Flashover Voltage (FOV) is obtained for the range of SDD (0 to 11mg/cm²) under LI and SI voltages, by adopting step stress method [14]. In the present study, flashover voltages are measured by carrying out the discharge tests at different spatial locations on the surface of the polluted sample [19-21]. This is carried out to minimize the variation in surface condition (such as surface roughness, distribution of polluted layer and thickness of the test specimen) of polluted GFRP. It is observed that the flashover voltage of GFRP is drastically reduced on deposition of pollutant (kaolin clay) on the surface of GFRP material under LI/SI, irrespective of its polarity. It is also observed that the FOV of electrode gap reduces with increase in SDD. The characteristics is the same irrespective of the polarity of the applied voltage. In general, the FOV is high under LI compared with SI voltage. In addition, the FOV is high under negative LIV compared with positive LIV. The variation in flashover voltage depends on many factors which includes salt density distribution on surface of the sample, surface condition of salt deposit, electrode gap distance etc. In general, it is observed that SDD and FOV show inverse relationship. Vasa *et al.* experimentally observed a reduction in flashover voltage in case of polluted wind turbine blade samples under lightning (2/50 μ s) and switching (250/2500 μ s) impulse voltages [22]. Danikas *et al.* showed that the flashover voltage decreases with increase in conductivity of the water droplet of the electrode gap on insulating materials under AC voltages [23]. Similar observations were reported by Douar *et al.* on deposition of polluted layer above an insulating surface [2]. Slama *et al.* showed that the critical flashover voltage of glass insulating surface depends on the pollution level and the polarity of lightning impulse voltage. The FOV is less under positive LIV than negative LIV

[11]. The results obtained by the author are on similar lines.

In case of switching impulse (SI) measurements, breakdown of an electrode gap occurs at a lower voltages compared to that of LI. This is mainly due to long wave front and tail times of SI voltage. Further, FOV measured under negative SIV is less compared with that of positive SIV. Similar characteristics were observed by Quisman *et al.* [24]. Madsen *et al.* showed that the negative polarity on high voltage electrode will result in lower breakdown strength of GFRP material under SIV [25]. Thickness of pollutant layer does not affect the breakdown voltage or flashover voltage as specified by Madsen *et al.* Based on the applied voltage magnitude and discharge current measured, amount of energy transferred to the GFRP samples during the discharge process is estimated under LI and SI voltage test. Energy deposit on samples with different salt deposit does not vary significantly, irrespective of polarity of applied voltage (LIV/SIV). It is also observed that the amount of energy deposited is high under SIV (irrespective of level of SDD and polarity of applied voltage) compared with LIV. Energy deposit value under SIV is higher than that of LIV due to wave shape of the applied voltage and duration of current flow. Hence the damage to the GFRP sample is expected to be significant.

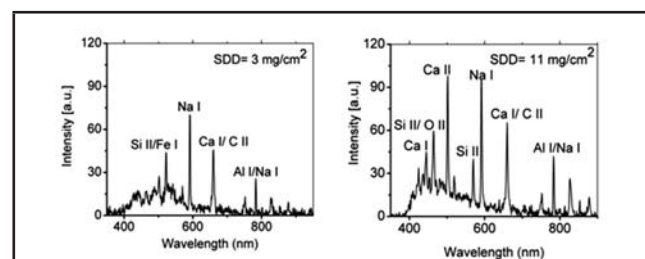


FIG. 2. TYPICAL OPTICAL EMISSION SPECTRA OBTAINED DURING DISCHARGE (POSITIVE LIGHTNING IMPULSE VOLTAGE): SDD OF 3MG/CM² AND SDD OF 11MG/CM².

Electric field strength between the electrodes gets intensified as the applied voltage rises towards its peak value. If the electric field stress on the test specimen exceeds its breakdown strength of the medium, localized discharges leading to flashover occurs. The flashover path is in which the discharge plasma (contains excited ions,

electrons, and neutral atoms) is formed. Within a short span of time, excited particles in the discharge plasma cools down and de-excite to their lower energy states by releasing equivalent energy in the form of radiation. On observing the plasma emission wavelengths in an optical range, elemental composition of the test specimen could be derived. The characteristic peak of emission lines observed in OES spectra of GFRP, kaolin clay deposited on GFRP material relates to its atomic composition [26]. Figure 2 show a typical optical emission spectra of polluted samples (SDD of 3 and 11 mg/cm²) under positive LI discharges. The optical emission spectra observed between the electrodes gaps under LIV/SIV, irrespective of polarity are the same.

Based on Figure 2, neutral (such as CaI, NaI) and singly ionized (such as CaII, SiII) atomic emission lines are observed. Very few doubly ionized atomic emission lines are observed in the spectra, since the ionization energy required to induce it is very high. As observed in Figure 2, characteristic peak at 588.99 nm relates to a neutral sodium atom (Na I, first ionization energy of 495.8 kJ/mol⁻¹) could be identified, which indicates the presence of contaminants. No chlorine peaks are observed, since the first ionization energy of chlorine (1251.2 kJ/mol⁻¹) is very high. When the discharge voltage was higher than that of the flashover voltage then the spectra of GFRP itself is observed with an addition of Na I line at 588.99 nm representing the propagation of discharge along the GFRP-contaminant boundary.

Temporal measurement of discharge plasma (Na I emission at 589 nm) are carried out. The Na I emission line profile at 589 nm in discharge plasma measured along with discharge current (using resistive short) are in correlation as shown in Figure 3 (a). The major part of the light is emitted during the breakdown and approximately during the first 500 ns and slowly decays. Descoeudreset *al.* observed that the optical emission profile from a electrical discharge machining plasma is in agreement with the discharge current profile [27]. The discharge plasma emission lifetime at 589 nm is estimated at 20% of the maximum emission intensity as shown in Figure 3 (b). Assuming the

tail portion of the Na I emission exponentially decays. Apparent Na I emission lifetime of 4 to 18 μ s and 24 to 96 μ s are observed for positive and negative switching impulse voltage profiles. Even though the discharge current decays fast, Na I emission in discharge plasma sustains for longer period in case of negative SIV and enhances the deterioration of GFRP material. Due to the salt contaminant, large magnitude of current is expected to flow along the conductive surface of the sample during discharge process. Particularly, in the case of switching impulse voltage, the contaminant surface with a low discharge impedance will allow more current and in turn heating of the surface will increase. Hence switching impulse voltage of both polarities induces a significant damage to the GFRP material compared to lightning impulse voltage.

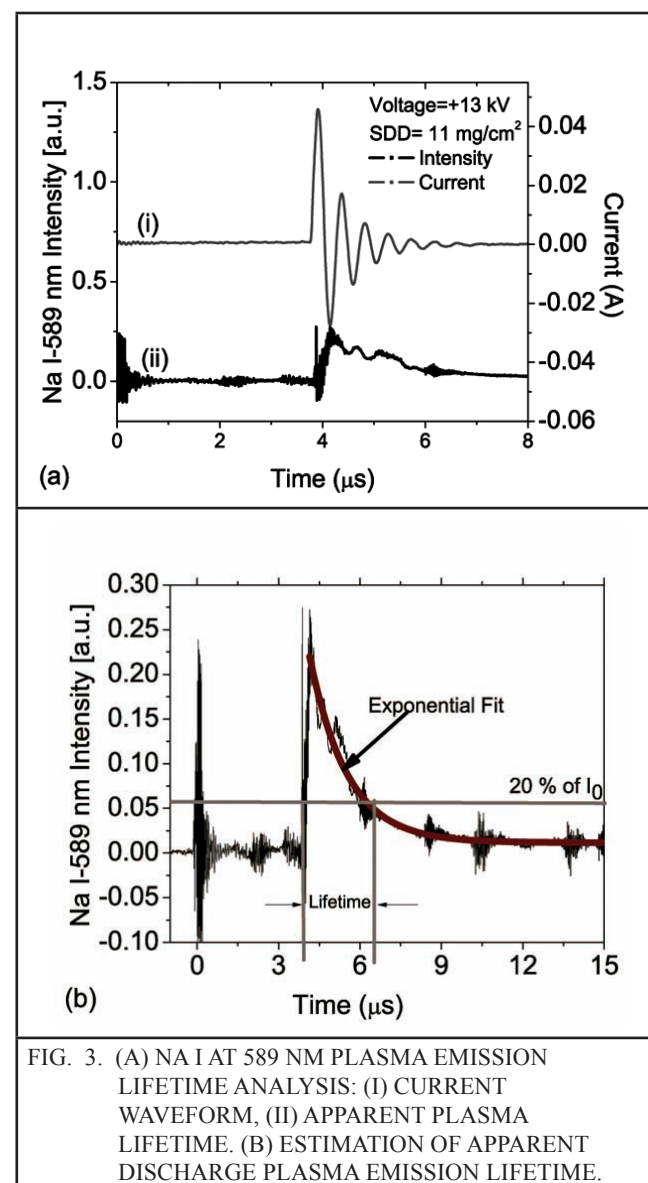


FIG. 3. (A) NA I AT 589 NM PLASMA EMISSION LIFETIME ANALYSIS: (I) CURRENT WAVEFORM, (II) APPARENT PLASMA LIFETIME. (B) ESTIMATION OF APPARENT DISCHARGE PLASMA EMISSION LIFETIME.

Electric field strength between the electrodes gets intensified as the applied voltage rises towards its peak value. If the electric field stress on the test specimen exceeds its breakdown strength of the medium, localized discharges leading to flashover occurs. The flashover path is in which the discharge plasma (contains excited ions, electrons, and neutral atoms) is formed. Within a short span of time, excited particles in the discharge plasma cools down and de-excite to their lower energy states by releasing equivalent energy in the form of radiation. On observing the plasma emission wavelengths in an optical range, elemental composition of the test specimen could be derived. The characteristic peak of emission lines observed in OES spectra of GFRP, kaolin clay deposited on GFRP material relates to its atomic composition [26]. Figure 2 show a typical optical emission spectra of polluted samples (SDD of 3 and 11mg/cm²) under positive LI discharges. The optical emission spectra observed between the electrodes gaps under LIV/SIV, irrespective of polarity are the same.

Based on Figure 2, neutral (such as CaI, NaI) and singly ionized (such as CaII, SiII) atomic emission lines are observed. Very few doubly ionized atomic emission lines are observed in the spectra, since the ionization energy required to induce it is very high. As observed in Figure 2, characteristic peak at 588.99 nm relates to a neutral sodium atom (Na I, first ionization energy of 495.8 kJ/mol⁻¹) could be identified, which indicates the presence of contaminants. No chlorine peaks are observed, since the first ionization energy of chlorine (1251.2 kJ/mol⁻¹) is very high. When the discharge voltage was higher than that of the flashover voltage then the spectra of GFRP itself is observed with an addition of Na I line at 588.99nm representing the propagation of discharge along the GFRP-contaminant boundary.

Temporal measurement of discharge plasma (Na I emission at 589 nm) are carried out. The Na I emission line profile at 589 nm in discharge plasma measured along with discharge current (using resistive short) are in correlation as shown in Figure 3 (a). The major part of the light is emitted during the breakdown and approximately during

the first 500 ns and slowly decays. Descoedreset al. observed that the optical emission profile from a electrical discharge machining plasma is in agreement with the discharge current profile [27]. The discharge plasma emission lifetime at 589 nm is estimated at 20% of the maximum emission intensity as shown in Figure 3 (b). Assuming the tail portion of the Na I emission exponentially decays. Apparent Na I emission lifetime of 4 to 18 μ s and 24 to 96 μ s are observed for positive and negative switching impulse voltage profiles. Even though the discharge current decays fast, Na I emission in discharge plasma sustains for longer period in case of negative SIV and enhances the deterioration of GFRP material. Due to the salt contaminant, large magnitude of current is expected to flow along the conductive surface of the sample during discharge process. Particularly, in the case of switching impulse voltage, the contaminant surface with a low discharge impedance will allow more current and in turn heating of the surface will increase. Hence switching impulse voltage of both polarities induces a significant damage to the GFRP material compared to lightning impulse voltage.

3.0 THEORETICAL ANALYSIS

Theoretical simulation studies based on electric field distribution are performed on GFRP samples and compared with results of electrical discharge experiments. In order to study the behaviour of lightning discharge on conducting and non-conducting surfaces, various approaches, such as Finite Difference Time Domain (FDTD) method, electrostatic field analysis method can be considered. Considering the simplicity, electrostatic field analysis is used to understand the spatial electric field distribution on GFRP sample without salt deposition (non-conducting surface) and with salt deposition (conducting surface).

3.1 Simulation Model

Figure 4 (a) show the geometrical model used for simulation studies. A square substrate with a surface area of 36cm² and thickness of 0.5cm is considered in the simulation studies. Properties

of the square substrate is specified as a glass fiber with a relative permittivity (ϵ_r) of 4.2 [28]. Above the square GFRP substrate, two eccentric cones (semi axis of 0.2cm and height of 5cm) shaped stainless steel electrodes are placed with a spacing of 1cm between them. Eccentric cones are selected in the model as a geometry for the electrodes in order to induce uniform electric field in the electrode gap. In order to test in polluted condition, a sheet of NaCl (0.1cm thick) with relative permittivity of 80 (corresponding to that of saline water) or 8000 (corresponding to conducting surface) is placed above the GFRP substrate [28], [29]. The whole geometry is enclosed by the air medium (10cm x10cm x8cm) with a relative permittivity of 1. The simulation is performed with an assumption that polluted layer is uniformly distributed over the GFRP material. Electrostatic field on the substrates are estimated using Gauss law on electric field and Poisson equation.

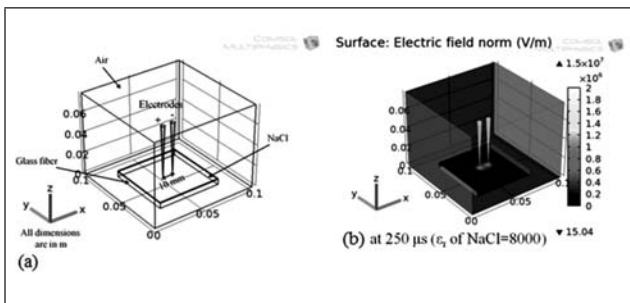


FIG. 4.(A) GEOMETRICAL MODEL USED FOR SIMULATION STUDIES, (B) ELECTRIC FIELD DISTRIBUTION ON POLLUTED GFRP UNDER SIV.

3.2 Results and Discussion

A 3D-finite element software package, COMSOL Multiphysics (version 4.0) is used for simulation studies. Lightning/Switching impulse voltages are generated using the following equation,

$$V(t) = V_p \times [\exp(-\alpha_1 t) - \exp(-\alpha_2 t)] \quad ..(1)$$

where V_p is the peak voltage (18kV), α_1 and α_2 are used to determine the front and tail time of the impulse voltage. A typical electric field normal distribution on the polluted GFRP sample (ϵ_r of NaCl= 8000) under the application of SIV of

positive polarity at 250 μ s are shown in Figure 4(b). It is observed that the electric field at the interface of electrode tip and NaCl layer is intense and it gradually decreases as the spatial distance in XY plane from the electrode tip increases. It is observed that the maximum value of electric field is obtained at the interface of electrode tip and NaCl layer when the applied voltage reaches its peak value as shown in Figure 5. It is also observed that the field gets reversed at the electrode with lower potential. The electric field on the surface of polluted and non-polluted samples follows the profile of applied voltage.

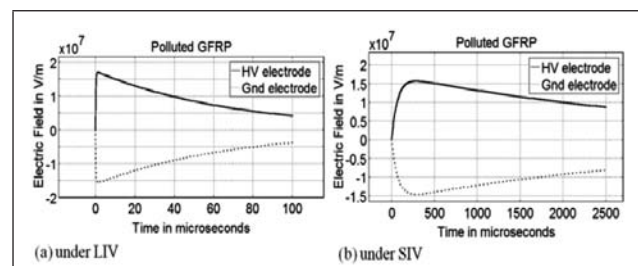


FIG.5. VARIATION OF ELECTRIC FIELD NEAR ELECTRODE TIP ON THE SURFACE OF POLLUTED GFRP (ϵ_r OF NaCl=8000): (A) UNDER LIV, (B) UNDER SIV.

Peak electric field at the electrode tip under positive LI and SI are summarized in Table. 1. It is observed that the electric field peak value differs for the LI and SI voltage profiles. Peak electric field intensity at the surface of virgin/polluted GFRP under LI is high compared to that of SI. It is observed that the electric field induced on the polluted GFRP sample is high compared to that of non-polluted GFRP. It is also observed that the peak value of electric field does not vary significantly for polluted layer with different permittivity's (ϵ_r of 80 or 8000). Under high electric field stress, the probability of discharge initiation is high. This study represents that the discharge can get initiated even at a lower voltage in the presence of salt layer compared to that of virgin GFRP. Similar observations have been recorded in our flashover voltage studies. Theoretical simulation studies clearly show that the flashover voltage reduces with increase in salt deposit density. Naka *et al.* showed that the electric field is intensified under polluted condition and maximum electric field intensity at

the wind turbine blade tip is approximately five times greater than the non-polluted blade [29].

TABLE 1

PEAK ELECTRIC FIELD (V/M) NEAR ELECTRODE TIP UNDER TRANSIENT VOLTAGES

TRANSIENT VOLTAGES	GLASS FIBER	POLLUTED GLASS FIBER
LIV	1.50×10^7	1.70×10^7
SIV	1.39×10^7	1.57×10^7

4.0 CONCLUSION

Electrical discharge measurement combined with Optical Emission Spectroscopy (OES) technique is proposed and demonstrated to study the influence of pollutant (salt deposit) on the GFRP material under Lightning Impulse (LI)/Switching Impulse (SI) voltages of both polarities. Damage to the GFRP material is found to be significant with an increase in the concentration of pollutant and also on application of switching impulse voltages (winter lightning). Optical Emission Spectroscopy (OES) studies show that the Na I emission line at 588.99nm could be identified for samples with different pollution level. Na I emission (589nm) in discharge plasma sustains for longer period in case of negative SIV, which represent that the surface temperature induced due to discharge sustains for longer period and enhances the deterioration of GFRP material. Electrostatic field analysis shows that the electric field induced on the polluted GFRP sample is high compared to that of non-polluted GFRP, irrespective of wave shape and polarity. Under high electric field stress, the probability of discharge initiation is high. This represents that the discharge can initiate even at a lower voltage in the presence of salt layer compared to that of virgin GFRP. Experimental observations using optical emission spectroscopy technique are qualitatively in agreement with the electrical discharge measurements. Hence OES technique can also be utilized to study about the contaminants in practical insulators.

ACKNOWLEDGMENTS

This work is supported by the grant-in aid from the DST (SR/S3/EECE/0115/2010).

REFERENCES

- [1] S. Chandrasekar, C. Kalaivanan, G. C. Montanari and A. Cavallini, "Partial discharge detection as a tool to infer pollution severity of polymeric insulators", *IEEETrans. Dielectr.Electr.Insul.*, Vol. 17, pp. 181-188, 2010.
- [2] M. A. Douar, A. Mekhaldi and M. C. Bouzidi, "Flashover process and frequency analysis of the leakage current on insulator model under non-uniform pollution conditions", *IEEETrans. Dielectr.Electr.Insul.*, Vol. 17, pp. 1284-1297, 2010.
- [3] I. L. Hosier, M. S. AbdRahman, A. S. Vaughan, A. Krivda, X. Kornmann and L. E. Schmidt, "Comparison of laser ablation and inclined plane tracking tests as a means to rank materials for outdoor HV insulators", *IEEETrans. Dielectr. Electr.Insul.*, Vol. 20, pp. 1808-1819, 2013.
- [4] A. Mekhaldi, D. Namane, S. Bouazabia and A. Beroual, "Flashover of discontinuous pollution layer on HV insulators", *IEEETrans. Dielectr.Electr.Insul.*, Vol. 6, pp. 900-906, 1999.
- [5] B. Moula, A. Mekhaldi and M. Tegar, "Evaluation of insulator's energy under uniform pollution condition", 2nd *IEEEEnergyconConf.*, pp. 975-978, 2012.
- [6] B. Moula, A. Mekhaldi, M. Tegar and A. Haddad, "Characterization of discharges on non-uniformly polluted glass surfaces using a wavelet transform approach", *IEEETrans. Dielectr.Electr.Insul.*, Vol. 206, pp. 1457-1466, 2013.
- [7] G. Zhicheng and C. Renyu, "Calculation of DC and AC flashover voltage of polluted insulators", *IEEETrans. on Electr.Insul.*, Vol. 25, pp. 723-729, 1990.

- [8] H. H. Woodson and A. J. Mcelroy, "Insulators with contaminated surfaces, Part II- Modeling of discharge mechanisms", *IEEETrans. on Power Apparatus and Systems*, Vol. 89, pp. 1858-1867, 1970.
- [9] K. L. Chrzan, H. Schwarz and H. Hausler, "Effect of impulse polarity on the flashover voltage of polluted cap and pin insulators", *Proc. of 16th Intern. Symp.onHigh Voltage Engineering*, pp. 1-5, 2009.
- [10] M. A. Douar, A. Mekhaldi and M. C. Bouzidi, "Investigations on leakage current and voltage waveforms for pollution level monitoring under wetted and contaminated conditions", *IETSci. Meas. Technol.*, Vol. 59, pp. 67-75, 2011.
- [11] M. El-A. Slama, A. Beroual and H. Hadi, "Influence of the linear non-uniformity of pollution layer on the insulator flashover under impulse voltage-estimation of the effective pollution thickness", *IEEETrans. Dielectr.Electr.Insul.*, Vol. 18, pp. 384-392, 2011.
- [12] N. Dhahbi Megriche and A. Beroual, "Dynamic model of discharge propagation on polluted surfaces under impulse voltages", *IEEProc. Gener.Transm. Distrib.*, Vol. 147, pp. 279-284, 2000.
- [13] SH. Taheri, A. Gholami and M. Mirzaei, "Study on the behavior of polluted insulators under lightning impulse stress", *Electric power components and systems*, Vol. 37, pp. 1321-1333, 2009.
- [14] "IEC 60507 standard: Artificial pollution test on high voltage insulators to be used in AC systems", *CEI/JEC 507:1991*, 1991.
- [15] V. Cooray, "The lightning flash", *IEEPower and Energy Series 34*, London, 2003.
- [16] "IEC publication 60: High-voltage test techniques: Part 1: General definitions and test requirements, second edition, 1989-11. Part 2: Measuring systems, second edition, 1994-11", 1994.
- [17] "IEEESTD 4-1995: IEEE standard techniques for high-voltage testing.", 1995.
- [18] "IEC-60112-Method for the determination of the proof and the comparative tracking indices of solid insulating material", *BS EN 60112: 2003*, 2003.
- [19] V. Sathiesh Kumar, N. J. Vasa and R. Sarathi, "Study on pollution performance on a wind turbine blade using OES technique for lightning and switching impulse voltage profiles", *JurnalTeknologi (Sciences and Engineering)*, Vol. 64, pp. 63-68, 2013.
- [20] V. Sathiesh Kumar, N. J. Vasa and R. Sarathi, "Detecting salt deposition on a wind turbine blade using laser induced breakdown spectroscopy technique", *J. Applied Physics A*, Vol. 112, pp. 149-153, 2013.
- [21] V. Sathiesh Kumar, NileshJ. Vasa, R. Sarathi, Daisuke Nakamura and Tatsuo Okada, "Understanding the discharge activity across GFRP material due to salt deposit under transient voltages by adopting OES and LIBS technique", *IEEETrans. Dielectr. Electr.Insul.*, Vol. 21, pp. 2283-2292, 2014.
- [22] N. J. Vasa, T. Naka, S. Yokoyama, A. Wada and A. Asakawa, "Experimental study on lightning attachment manner considering various types of lightning protection measures on wind turbine blades", *Proc. Intern. Conf. on Lightning Protection (ICLP)*, Kanazawa, Japan, pp. 1483-1487, 2006.
- [23] M. G. Danikas, R. Sarathi, P. Ramnalis and S. L. Nalmpantis, "Analysis of polymer surface modifications due to discharges initiated by water droplet under high electric fields", *World Academy of Science, Engineering and Technology*, Vol. 50, pp. 871-876, 2009.
- [24] S. Quisman, M. Steen Aanderson, J. Holboell and M. Henriksen, "GFR-materials resistance to lightning with respect to lightning protection of windmill wings", *Intern. Conf. on Lightning and Static Electricity*, pp. 1-7, 2003.
- [25] S. F. Madsen, F. M. Larsen, L. B. Hansen and K. Bertelsen, "Breakdown tests of glass fiber reinforced polymers (GFRP) as a part

- of improved lightning protection of wind turbine blades", IEEE Intern.Sympos.Electr. Insul.(ISEI), pp. 484-491, 2004.
- [26] "Nist handbook of basic atomic spectroscopic data, <http://physics.nist.gov/physrefdata/handbook/index.html>", 2013.
- [27] A. Descoedres, CH. Hollenstein, R. Demellayer and G. Walder, "Optical emission spectroscopy of electrical discharge machining plasma", Journal of Physics D, Applied Physics, Vol. 37, pp. 875-882, 2004.
- [28] T. Naka, N. J. Vasa, S. Yokoyama, A. Wada and S. Arinaga, "Investigation between electrostatic field analysis and results of lightning discharge experiment with wind turbine blades", Intern. Conf. on Lightning Protection (ICLP), Kanazawa, Japan, pp. 1-5, 2006.
- [29] D. H. Gadani, V. A. Rana, S. P. Bhatnagar, A. N. Prajapati and A. D. Vyas, "Effect of salinity on the dielectric properties of water", Indian Journal of Pure and Applied Physics, Vol. 50, pp. 405-410, 2012.

